Cement and Concrete Composites 120 (2021) 104035

Contents lists available at ScienceDirect

Cement and Concrete Composites

journal homepage: http://www.elsevier.com/locate/cemconcomp

Rheological behavior of cement paste with nano-Fe_3O_4 under magnetic field: Magneto-rheological responses and conceptual calculations

Dengwu Jiao [a,b], Karel Lesage [a], Mert Yucel Yardimci [a], Khadija El Cheikh [a], Caijun Shi [b], Geert De Schutter [a,*]

[a] Magnel Laboratory for Concrete Research, Department of Structural Engineering and Building Materials, Ghent University, 9052 Ghent, Belgium
[b] Key Laboratory for Green and Advanced Civil Engineering Materials and Application Technology of Hunan Province, College of Civil Engineering, Hunan University, Changsha 410082, China

ARTICLE INFO

Keywords:
Active rheology control (ARC)
Active stiffening control (ASC)
Structural build-up
Magnetic field
Nano-Fe_3O_4

ABSTRACT

The magneto-rheological responses of cement paste with nano-Fe_3O_4 particles are experimentally investigated. The estimated magneto-dynamic force between two neighboring nanoparticles and equilibrium movement velocity of the nanoparticles in cement-based suspensions are calculated. Results show that the nanoparticles have a potential to move to form magnetic clusters when a magnetic field is applied, which creates a sort of agitation effect breaking down the early C-S-H links between cement particles, and thus the corresponding suspensions exhibit liquid-like behavior immediately after applying the magnetic field. The solid-like property of the studied suspensions becomes more dominant with magnetizing time due to the formation of magnetic clusters and the reconstruction of C-S-H bridges. The rheological properties of paste medium exert significant influences on the magneto-rheological responses of cement paste containing nano-Fe_3O_4 particles. It is revealed that the calculated magnetic yield parameter and nanoparticle movement velocity are useful relevant indicators to evaluate the magneto-rheological effect of cementitious paste.

1. Introduction

The engineering application process of concrete includes transporting, pumping and formwork casting. Each process is a significant factor influencing the properties of fresh and hardened concrete. However, for a specific concrete mixture proportion, once the concrete is prepared, its properties cannot be further adjusted nor controlled post-mixing. The concrete will be transported, pumped and cast according to its mixture-dependent properties, requiring appropriate processing methods. Many conflicts and contradictions in requirements of fresh concrete performances exist in different operation processes. For example, low thixotropic structural build-up is needed to overcome the major problem in resuming pumping operations after a short interruption (e.g. due to the delay of the concrete truck) [1] and to improve the interface properties during multi-casting process [2]. In contrast, a higher structuration rate of fresh concrete is beneficial for reducing formwork pressure during casting [3,4]. In this context, an innovative casting concept "SmartCast" has been proposed by De Schutter [5,6] to overcome the aforementioned problems. By active rheology control (ARC) and active stiffening control (ASC) of fresh concrete, pumping and casting operations could be better controlled and become more reliable.

Magnetorheological (MR) fluids are kinds of smart materials, consisting of magnetic particles, carrier fluid and additives. In the absence of external magnetic field, the magnetic particles are randomly distributed in the carrier fluid. After the application of an external magnetic field, the magnetic particles align along the direction of the magnetic field and form chain-like or columnar structures, resulting in higher elastic behavior [7,8]. After removing the external magnetic field, the chain-like structures break down and the MR fluid reversibly changes from semi-solid to liquid state. However, due to the significant difference in density between magnetic particles and carrier fluid, particle sedimentation has become a main limitation of industrial applications of conventional MR fluids. One of the potential approaches to improve the stability of MR fluids is using a yield stress carrier fluid [9–12]. Fresh cement paste is usually regarded as a concentrated suspension with yield stress [13–15]. A stable cement-based MR fluid could be obtained using fresh cement paste as the carrier, and meanwhile, the rheological

* Corresponding author.
E-mail address: geert.deschutter@ugent.be (G. De Schutter).

https://doi.org/10.1016/j.cemconcomp.2021.104035
Received 5 October 2020; Accepted 24 March 2021
Available online 31 March 2021

properties of the cement paste would become controllable. Some preliminary results about the effect of magnetic field on the properties of cement-based materials can be found in literature. For example, the pumpability of fresh concrete seems to be somewhat improved by applying an electromagnetic field [16]. By exposing fresh steel chip-reinforced concrete specimen into an alternating magnetic field, the steel chips act as a vibrator and the compaction of concrete can be facilitated [17]. More information about the application of external signals to control concrete properties can be found in Ref. [5]. Nevertheless, there is currently no comprehensive understanding of the MR behavior of cementitious materials, especially at the initiation of the magnetic field.

Ferroferric oxide (Fe_3O_4) is a ferromagnetic material with Fe^{2+} and Fe^{3+}, and the magneto dipoles can be aligned along the direction of an external magnetic field. The addition of nano-Fe_3O_4 particles in cement-based materials has attracted extensive interest [18]. The nano-Fe_3O_4 particles, on the one hand, fill the voids between cement particles, leading to a denser suspension system. On the other hand, the nanoparticles provide nuclei for cement hydration products [19]. As a consequence, the hydration reaction of cementitious materials is accelerated with the addition of nano-Fe_3O_4 particles, and thus the early age mechanical properties are enhanced [20,21]. Moreover, the Fe available in the cement-based materials because of the addition of nano-Fe_3O_4 has a potential to form Kuzel salts and Fe-ettringite which accumulate in the pores and voids between cement particles, resulting in an enhanced microstructure and higher electrochemical stability [22]. Mansouri et al. [23] found that the replacement of 2% cement with nano-Fe_3O_4 particles dramatically reduced the percentage of water adsorption and improved the resistance of chloride ion permeation, providing a potential extension of service life of submerged structures. From a fresh performance point of view, cement paste containing nano-Fe_3O_4 particles possesses fluid and magnetic properties at the same time. This provides a potential reasonable method to control the rheological behavior of cement paste by applying external magnetic fields.

Our previous publications [24,25] presented some preliminary findings about the rheological behavior of cement paste under external magnetic field. The structural evolution of cement paste under time-varying magnetic fields was also studied. In the current study, the structural build-up of cement paste with nano-Fe_3O_4 particles under constant magnetic field is experimentally investigated using small amplitude oscillatory shear (SAOS) technique. The magneto-rheological responses illustrated by the relationship between storage modulus, loss modulus and phase angle are discussed. The influences of cement paste medium on the magneto-rheological responses are also examined. The hypothesis concerning the underlying mechanisms is verified by estimating the magneto-dynamic force between two neighboring nanoparticles and the movement velocity of the nanoparticles in cement-based suspensions, based on some conceptual approach.

2. Experimental program

2.1. Raw materials

Ordinary Portland cement (OPC) CEM I 42.5 N conforming to EN 196–1 [26] is used in this study. The chemical composition and particle size distribution are respectively shown in Table 1 and Fig. 1. The specific gravity of the Portland cement is 3.15. Spherical Iron Oxide nano-Fe_3O_4 particles (MNPs) with Fe_3O_4 purity higher than 98% (from US Research Nanomaterials, Inc) are used. The particle size and relative density of the nano-Fe_3O_4 particles supplied by the manufacturer are 20–30 nm and 4.95, respectively. The curves of magnetization versus magnetic field strength of the cement and nanoparticles, obtained from a vibrating sample magnetometer (VSM), are shown in Fig. 2. The saturation magnetization of Portland cement particles and nano-Fe_3O_4 particles are 0.59 emu/g and 49.48 emu/g, respectively. The extremely low magnetization value of the cement particles means that the response of pure cement paste to an external magnetic field can be neglected [27,28]. A commercial polycarboxylate ether superplasticizer (PCE) (MasterGlenium 51) is used. All samples are prepared using de-ionized water.

Table 1
Chemical composition of the Portland cement.

Components	% by mass
SiO_2	19.6
Al_2O_3	4.88
Fe_2O_3	3.14
CaO	63.2
MgO	1.8
SO_3	2.9

2.2. Mixing procedure

Five cement pastes were prepared as the medium and the nano-Fe_3O_4 particles content was fixed at 3% by weight of the cement paste (i.e. cement + water). A mass of 20 g of cement was used for each sample. The mixture proportions of the cement pastes with nano-Fe_3O_4 particles are shown in Table 2. The cement paste was mixed using a rotational rheometer (MCR 52, Anton Paar) with a helix geometry, which provides repeatable initial state of paste samples with same mixture proportion. The details of the geometric parameters of the helix geometry and the mixing procedure can be found in Ref. [25].

2.3. Testing methods

A rotational parallel plate rheometer (MCR 102, Anton Paar) with magneto-rheological device (MRD) was used for the rheological test. The diameter of the plate is 20 mm and the gap between the upper and lower plates is fixed at 1 mm. A homogeneous magnetic field vertical to the plates can be applied to the sample by inputting specific current. During the rheological tests, the temperature of all samples was controlled at 20 ± 0.5 °C. Rheological tests were repeated three times using fresh samples.

The testing protocol for evaluating the structural build-up of the cement pastes is presented in Fig. 3. The magnetic field was applied to the sample at the beginning of the oscillatory time sweep test, and the field strength used in this study included 0 T and 0.5 T. During the strain sweep test, the shear strain logarithmically swept from 0.0001% to 10% at constant frequency of 2 Hz. The strain amplitude and frequency during the time sweep test were 0.001% (within the linear viscoelastic region (LVER)) and 2 Hz, respectively.

Moreover, an additional flow curve test was conducted using fresh

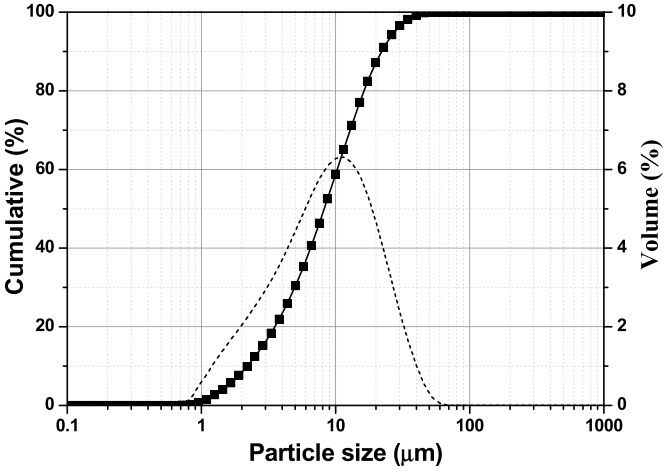

Fig. 1. Particle size distribution of the Portland cement.

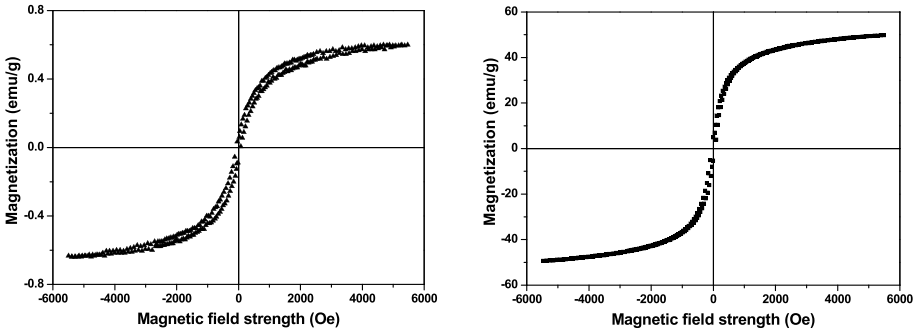

(a) Portland cement (b) Nano-Fe_3O_4 particles

Fig. 2. Magnetization versus magnetic field strength curves (1 T = 10000 Oe).

Table 2
Mixture proportions of cement pastes used in this study.

No.	Cement (g)	Water (g)	MNPs (g)	PCE (g)
0.4	20	8	0.84	0
0.35	20	7	0.81	0
0.35 + 0.2%PCE	20	7	0.81	0.04
0.35 + 0.4%PCE	20	7	0.81	0.08
0.35 + 0.6%PCE	20	7	0.81	0.12

samples to measure the rheological parameters of cement pastes in the absence of magnetic field. The key parameters during the shear curve test are as follows. During the pre-shearing process, the shear rate and duration were respectively 100 s^{-1} and 30 s. Afterwards, the shear rate logarithmically decreased from 100 s^{-1} to 0.1 s^{-1} within 100 s, and the shear stress and shear rate were recorded every second.

3. Experimental results

3.1. Rheological properties of cement pastes without magnetic field

The storage modulus (G′) and loss modulus (G″) obtained during the oscillatory strain sweep test are used to evaluate the viscoelastic behavior of the cement pastes in the absence of external magnetic field. The storage modulus, related to the energy stored in each cycle, describes the elastic behavior of the system. The loss modulus characterizes the viscous property of the paste, which is proportional to the energy dissipated in each measuring cycle. A typical oscillatory strain sweep testing result of the cement paste with w/c of 0.4 and nano-Fe_3O_4 of 3 wt% is displayed in Fig. 4. At relatively low shear strain, the storage modulus and loss modulus showed plateau behavior (LEVR), and the storage modulus was higher than the loss modulus, indicating that the solid-like property of the cement paste dominates the liquid-like property. At shear strain higher than a critical strain, the storage modulus and loss modulus started to decline, indicating the breakage of C-S-H links between cement particles. The crossover point between the storage modulus and loss modulus at shear strain of ~2% represents the beginning of viscous property domination under oscillatory amplitude sweeping. The aforementioned critical strain can be determined by the point where the storage modulus deviates 10% from the plateau [29,30]. The elastic stress at the critical strain is defined as elastic limit yield stress, which can be calculated by Eq. (1). The magnitude of the elastic limit yield stress can be used to characterize the intensity of C-S-H contacts between cement particles.

$$\tau_{c,ys} = \gamma_c \cdot G' \quad (1)$$

where $\tau_{c,ys}$ is the elastic limit yield stress (Pa), γ_c is the critical strain (%), and G' is the storage modulus at critical strain (Pa).

Fig. 5 shows a representative flow curve of the cement paste with w/c of 0.4 and nano-Fe_3O_4 content of 3%. With the decrease of shear rate, the measured shear stress first slowly decreased and then dramatically decreased. This indicates that the cement paste showed noticeable shear thinning behavior at the selected shear rate region, which is consistent with [31–33]. At extremely low shear rates (e.g. less than 1 s^{-1}), a slight increase in shear stress was observed from the inserted enlarged view in Fig. 5. This can be explained by the competition between attractive particle interactions and hydrodynamic forces. At extremely low shear rates, the attractive forces between solid particles dominate the repulsive ones and hydrodynamic forces. Agglomerates and clusters between

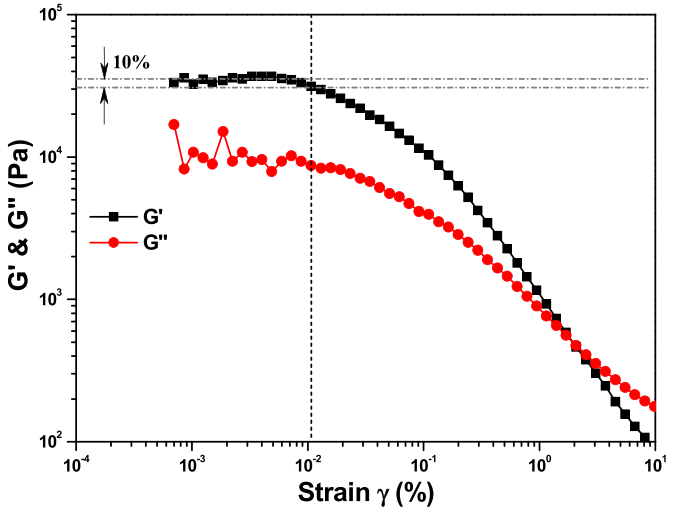

Fig. 4. Typical oscillatory strain sweep test results of cement paste (w/c = 0.4, MNPs = 3%).

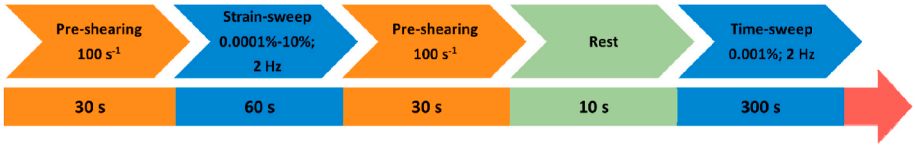

Fig. 3. Rheological testing protocols used in this study.

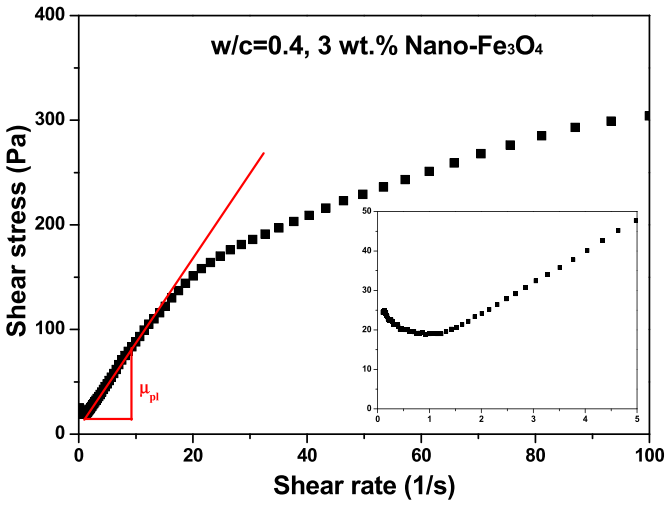

Fig. 5. Typical shear curve of cement paste (w/c = 0.4, MNPs = 3%).

particles, especially nano-Fe_3O_4 magnetic particles, are formed, leading to a slightly higher measured shear stress. Furthermore, the interparticle contacts might exert a significant resistance to the shear flow at low shear rates [34]. As a result, the slight increase in shear stress at low shear rates was recognized.

The main properties of the cement pastes obtained from the oscillatory strain sweep test and shear curve test are summarized in Table 3. Plastic viscosity at linear low shear rate region (η_{pl}) was selected to characterize the dynamic rheological behavior. The stiffness of cement paste was expectedly increased with the decrease of water content (i.e. w/c). At fixed w/c, both the elastic limit yield stress and the viscosity at low shear rates were increased after adding 0.2% PCE. The slight increase in stiffness of cement paste with low PCE addition can be found in Refs. [35,36]. This unexpected aberration in this study can be explained by the potential deagglomeration of nanoparticle clusters. At w/c of 0.35, some nano-Fe_3O_4 particles might aggregate to clusters in the cement paste due to the low water content. After adding small dosage of PCE (0.2%), the large nano-Fe_3O_4 clusters could be broken to small clusters or individual nanoparticles, improving the dispersion of the solid particles, and thus requiring more water to coat the surface of the nano-Fe_3O_4 particles. As a result, free water with lubricating effect was decreased. Besides, the addition of PCE increases the viscosity of the interstitial solution and thus the adhesion between particles. Consequently, the stiffness of the cementitious paste increased with the addition of 0.2% PCE. With the continuous increase of PCE content, the stiffness of cement paste was significantly decreased, as reflected by the decrease in the storage modulus at linear viscoelastic region. Remarkably, the critical strain exhibited an increasing behavior with the addition of PCE, which is consistent with [37,38]. As a result, the elastic limit yield stress of cement pastes with PCE was higher than that of cement pastes without PCE. It should be mentioned that the high viscosity of Mix. 0.35 + 0.4%PCE at low shear rates could possibly be attributed to the increase of shear thinning intensity due to the presence of PCE, showing a high resistance to the shearing.

Table 3
Main properties of the cement pastes in the absence of magnetic field.

Mix.	G' (LEVR) / (Pa)	γ_c / (%)	$\tau_{c,ys}$ / (Pa)	η_{pl} / (Pa.s)
0.4	3.48×10^4	0.013	4.52	7.21
0.35	4.64×10^4	0.0129	5.99	10.65
0.35 + 0.2%PCE	1.44×10^5	0.0416	59.91	20.00
0.35 + 0.4%PCE	3.36×10^4	0.134	45.03	28.89
0.35 + 0.6%PCE	3.64×10^3	0.528	19.22	9.44

Note: G' (LEVR) is the storage modulus at linear viscoelastic region. γ_c is the critical strain. $\tau_{c,ys}$ is the elastic limit yield stress. η_{pl} is the viscosity at linear low shear rate region.

3.2. Magneto-rheological responses of cement paste with nano-Fe_3O_4

3.2.1. Evolution of viscoelastic properties

The developments of storage modulus and loss modulus of the cement paste with w/c of 0.4 and nano-Fe_3O_4 particles of 3 wt% are shown in Fig. 6. In the absence of magnetic field, the storage modulus was always higher than the loss modulus, indicating that the solid-like property dominates the liquid-like behavior during the entire time-sweep test. Both storage modulus and loss modulus increased over time, but the storage modulus showed relatively high increase rate. This points to a gradual enhancement of the solid-like property, probably due to the multiple effects of flocculation, thixotropy and slight chemical hydration reactions [38,39]. Strong inter-particle interaction forces, dominating the Brownian motion and inertial forces [38,40], lead to formation of flocculated structures. This is reflected by the remarkable increase in the storage modulus at very early age. Furthermore, C-S-H links and bridges between cement particles are continuously formed with the progress of cement hydration. As a result, the rigidity and stiffness of the cement-based suspensions are consolidated, exhibiting a gradual increase in storage modulus with nearly constant increase rate.

In the presence of an external magnetic field, it can be observed that the cement paste containing nano-Fe_3O_4 particles showed obvious magneto-responses, as applying magnetic field evidently affected the evolution of the storage modulus and loss modulus. More specifically, the storage modulus showed a slight increase immediately after applying the magnetic field and then dramatically increased with magnetization time. This can be explained by the formation of magnetic clusters of nano-Fe_3O_4 particles under magnetic field [41]. The increase rate of the storage modulus slowed down after about 150 s, nevertheless reaching G' values that are significantly higher than that obtained without magnetic field. The linear increase of storage modulus represents the enhancement of C-S-H connections between flocculated structure due to chemical hydration of cement particles [37,42]. The equivalent increase rate of the storage modulus at steady state indicates that applying the external magnetic field has negligible influence on the intensity of C-S-H links between cement particles.

The loss modulus of cement paste containing nano-Fe_3O_4 particles also showed distinct evolution trends in the absence and presence of the external magnetic field. Without the magnetic field, the loss modulus slightly increased with increasing magnetization time. In the presence of the external magnetic field, however, the loss modulus increased first and then gradually decreased. Moreover, the loss modulus of the cement

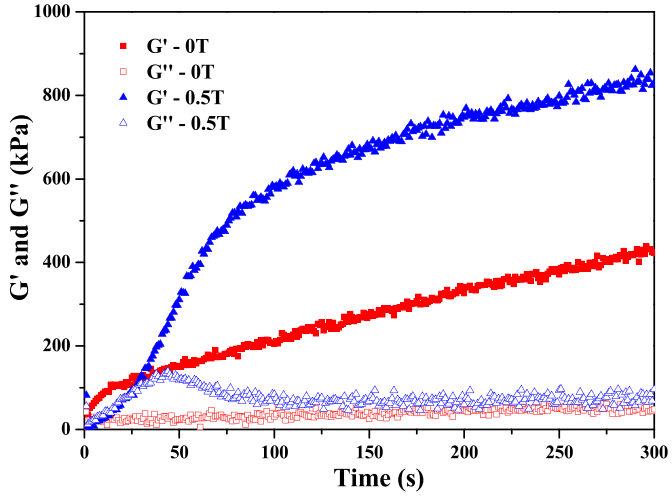

Fig. 6. Evolution of storage modulus and loss modulus of cement paste (w/c = 0.4, MNPs = 3%).

paste was even higher than the storage modulus at very early age. This can be attributed to the micro-movement of the nanoparticles under external magnetic forces, which will be discussed through the relationship between storage modulus, loss modulus and phase angle.

3.2.2. Relationship between G′, G″ and phase angle

In the presence of an external magnetic field of 0.5 T, the representative evolutions of storage modulus (G′), loss modulus (G″) and phase angle of the cement paste with w/c of 0.4 and nano-Fe_3O_4 particles of 3 wt% are shown in Fig. 7.

At the initiation of the external magnetic field, i.e. t_0, the loss modulus was higher than the storage modulus and the phase angle was close to 80°. This indicates that the cement paste showed almost totally liquid-like behavior immediately after initiation of the external magnetic field, which is consistent with our previous study [25] as well as with Nair and Ferron [43]. This can be attributed to the displacement and movement of magnetic nanoparticles in cement paste medium under external magnetic field. Without the external magnetic field, the magnetic nanoparticles can be regarded as randomly distributed in cement paste medium. When the magnetic field is applied, the nano--Fe_3O_4 particles will be magnetized and the magnetic dipoles have a potential to form chains and/or clusters in a very short time. During their displacement to form the magnetic clusters, the nanoparticles create a sort of mechanical micro-agitation, destroying the C-S-H bridges between cement particles, as schematized in Fig. 8 (a). Moreover, some possibly entrained water in the agglomerated cement clusters is released, which increases the content of free water. As a result, a more dispersed state is obtained after initiation of the external magnetic field. It should be noted here that most probably not all the nano-Fe_3O_4 particles will contribute to the formation of the clusters, due to the resisting viscoelastic properties of the cement-based medium.

With increasing magnetization time, the cement paste gradually transitions from viscous state to elastic state, where the capacity of energy stored gradually increases and simultaneously part of the mechanical energy dissipates. This is reflected by the rapid increase in storage modulus, the decrease in phase angle and the slight increase in loss modulus. This could be explained by the particles distribution, as depicted in Fig. 8 (b). On the one hand, part of the remaining nanoparticles in the interstitial solution try to move to join the clusters under the magnetic force, and meanwhile, the cement particles disturbed by the moving nanoparticles will try to reach new equilibrium positions, resulting in a slight increase in the loss modulus. On the other hand, the interactions between the magnetic clusters are improved, and new bridges and links between cement particles are gradually re-formed due to the colloidal interactions and cement hydration, which enhances the elastic property. At t_1, the storage modulus was equal to the loss modulus and the phase angle was 45°, indicating that the elastic-solid property starts to dominate the viscous-liquid property.

When the elastic-solid property reaches a threshold (t_2), the number of nanoparticles contributing to the clusters reaches the maximum, and the cement particles arrive at their final equilibrium positions, as represented in Fig. 8 (c). Therefore, the energy dissipation becomes limited, and the loss modulus reaches a maximum. With the continuous magnetization, the solid-like behavior evolves and the loss modulus starts to decline. After a sufficiently long period of magnetization (e.g. t_3), the cement-based suspensions possess enough elastic property and the deformation energy is hardly dissipated. This is reflected by the slight decrease in phase angle and loss modulus. Since the C-S-H links and bridges gradually evolve over time, as shown in Fig. 8 (d), the storage modulus gradually increases with magnetization time. Overall, for the cement paste containing nano-Fe_3O_4 particles, the application of an external magnetic field improves the liquid-like properties at very early age, and enhances the solid-like properties after enough long period of magnetization.

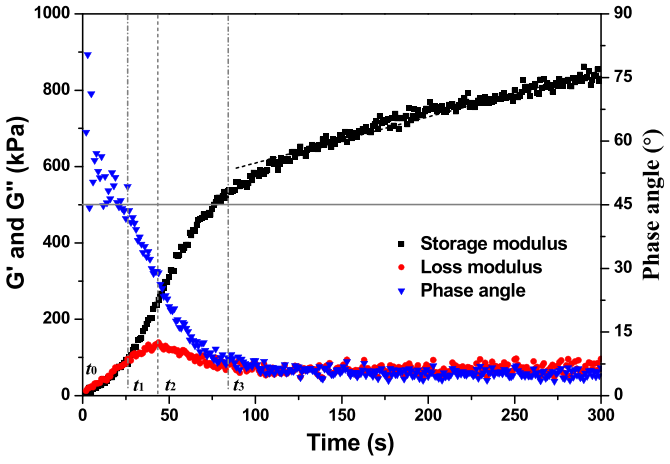

Fig. 7. Evolution of G′, G″ and phase angle for the cement paste under magnetic field of 0.5 T.

3.3. Effect of cement paste medium on magneto-rheological responses

Fig. 9 (a) presents the evolution of storage modulus and loss modulus of cement paste with w/c of 0.35, no PCE and nano-Fe_3O_4 of 3 wt%. For comparative analysis, Fig. 6 was modified to Fig. 9 (b) to keep same coordinates with Fig. 9 (a). Under zero magnetic field, the reduction in w/c significantly increased the magnitude of storage modulus, indicating higher stiffness of cement paste with lower water content. This can be attributed to the higher solid fraction and particle contacts. Furthermore, the cement paste with lower w/c showed a faster flocculated structural formation. Indeed, shorter time was required for the cement paste with w/c of 0.35 to reach a stable state of storage modulus, which is in agreement with [37]. Under an external magnetic field of 0.5 T, both cement pastes exhibited pronounced magneto-rheological behavior but with different intensities. The difference of the storage modulus at steady increase state obtained between 0 T and 0.5 T decreased with the reduction of w/c. Certainly, the storage modulus after magnetization for 300 s increased about 2.2 times and 1.2 times for the cement paste with w/c of 0.4 and 0.35, respectively. All the specific time points, including t_1 when storage modulus is equal to loss modulus, t_2 when loss modulus reaches a peak and t_3 when loss modulus starts to be stabilized, were shortened with the w/c of the cement paste medium decreasing from 0.4 to 0.35.

From the above results, it can be concluded that the cement paste with w/c of 0.4 showed more obvious magneto-rheological response than that with w/c of 0.35. This can be attributed to the relatively high stiffness of the cement paste with high solid concentration. According to Table 3, it can be seen that the elastic limit yield stress and viscosity of the cement paste with w/c of 0.35 (5.99 Pa and 10.65 Pa.s) were higher than that of cement paste with w/c of 0.4 (4.52 Pa and 7.21 Pa.s). This means that under a magnetic field with same strength, the cement paste with w/c of 0.35 exerts higher movement resistance to the nano-Fe_3O_4 particles to form magnetic clusters than the cement paste with w/c of 0.4. Therefore, the interactions between the formed magnetic clusters are lowered with the decrease of w/c. Overall, for the same nano-Fe_3O_4 particles concentration and without superplasticizer, the cement paste with higher solid fraction shows lower response to an external magnetic field.

Fig. 10 shows the influence of PCE dosage of cement paste medium on the evolution of storage modulus under w/c of 0.35 and nano-Fe_3O_4 content of 3 wt%. It should be mentioned that under zero magnetic field, the storage modulus of the cement paste with 0.2% PCE was higher than that of the cement paste without PCE (as can be seen by comparing Figs. 9 (a) and Fig. 10). This is in agreement with the oscillatory strain sweep test results in Table 3. Viewed as a whole, all the cement pastes with PCE seemed to exhibit unapparent responses to the external

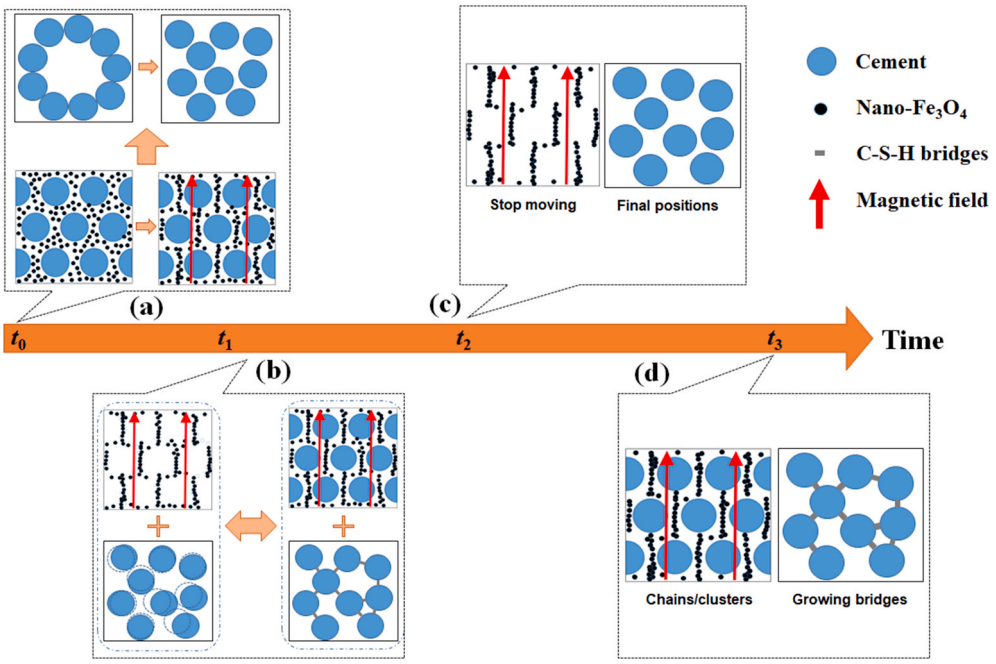

Fig. 8. Schematic diagram of distribution state of magnetic nanoparticles in cement paste with magnetization time.

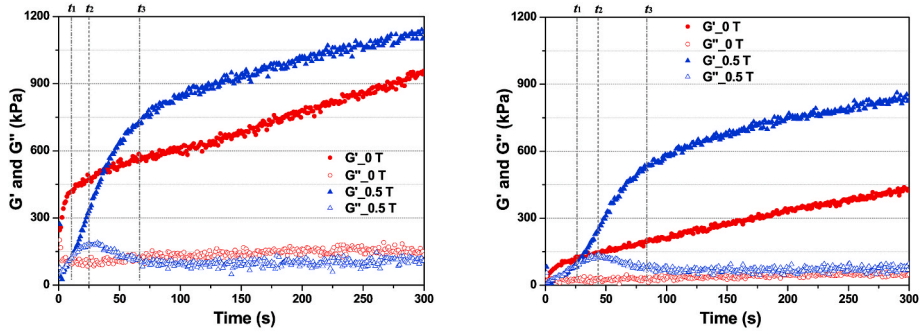

(a) w/c=0.35, no-PCE (b) w/c=0.4, no-PCE

Fig. 9. Evolutions of storage modulus and loss modulus of cement pastes with 3 wt% nano-Fe_3O_4.

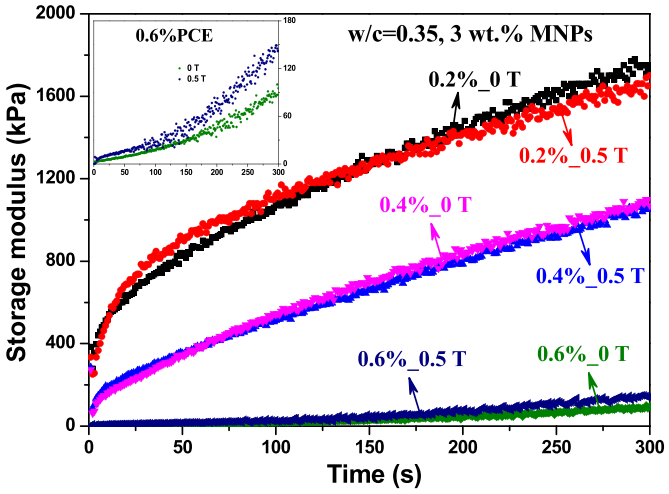

Fig. 10. Effect of PCE dosage of cement paste medium on evolution of storage modulus (w/c = 0.35, 3 wt% nano-Fe_3O_4).

magnetic field with 0.5 T. This can be explained by the high elastic limit yield stress and viscosity of the cement paste, as can be clearly found in Table 3. For the cement paste with 0.6% PCE, the storage modulus obtained under 0.5 T was slightly higher than that collected under zero magnetic field, especially after a longer period of magnetization (as can be seen from the inserted enlarged view in Fig. 10). This means that the cement paste with 0.6% PCE showed slight magneto-rheological response and magnetic clusters could be formed under the magnetic field. The slight increase of the storage modulus between 0 T and 0.5 T is probably due to the highly flowability of the suspension. Nevertheless, further research is required to study the interactions between nanoparticles and superplasticizer in cement-based suspensions under external magnetic field.

4. Validation: conceptual calculations

Under sufficiently strong magnetic field, the nano-Fe_3O_4 particles in cement-based suspension have a potential to move to form magnetic clusters. In order to start moving after applying the magnetic field, the magneto-dynamic force between adjacent nano-Fe_3O_4 particles should be higher than the resistance induced by the viscoelastic stress of the suspension. In this part, the estimated magneto-dynamic force and the

equilibrium movement velocity of the nanoparticles in the tested cement-based suspensions are tentatively calculated. It should be mentioned here that our aim is not to obtain the real numerical values of the magnetic force or movement velocity of nanoparticles in cement paste. Instead, hopefully the calculated parameters could provide some useful indicators for the rheological responses of a cementitious paste to an external magnetic field.

4.1. Magneto-dynamic force between nano-Fe_3O_4 particles

In the absence of an external magnetic field, the nano-Fe_3O_4 particles can be regarded as randomly distributed in cement paste medium. Assuming that all the nanoparticles have the same constant dipole moment under magnetic field, that is, neglecting the mutual magnetic induction between the nanoparticles, the interaction energy between two spherical particles can be expressed as Eq. (2) [11]:

$$U_{ij} = \frac{m^2\mu_0}{4\pi}\left(\frac{1-3\cos^2\theta}{r_{ij}^3}\right) \tag{2}$$

where U_{ij} is the interaction energy (J), m is the dipole moment (Am^2), μ_0 is the magnetic permeability of the medium (N/A^2), r_{ij} is the center distance between two magnetic nanoparticles (m), and θ is the angle between the center line and the magnetic field direction, as shown in Fig. 11. In case of cement paste as the medium, μ_0 can be considered equal to the value of vacuum ($4\pi \times 10^{-7}$ N/A^2). When the centers of two nanoparticles align along the direction of the magnetic field, i.e. $\theta = 0$, the magneto-dynamic force shows the maximum value:

$$F_{ij}\big|_{\theta=0} = \left|-\frac{dU_{ij}(\theta=0)}{dr_{ij}}\right| = \frac{3m^2\mu_0}{2\pi r_{ij}^4} \tag{3}$$

where the dipole moment m is related to the nature of the nanoparticles and the magnetic field strength, which can be expressed as:

$$m = \frac{\pi d^3 \rho M}{6} \tag{4}$$

where d is the average particle size of the nanoparticles (m). ρ and M are the density (kg/m^3) and the magnetization per unit mass (Am^2/kg) of the magnetic nanoparticles, respectively. It is to be mentioned that the calculated magnetic force is only intended as a representative measure for the effect of the applied magnetic field on two magnetic nanoparticles, instead of the real evolving force while moving in the paste. Indeed, nanoparticles in cement-based suspensions will experience mutual magnetic forces from surrounding particles. With the given expression, an estimation value is obtained that can be used as a quantitative parameter in further evaluation of the magneto-rheological behavior of the cement paste including magnetic nanoparticles. Comparing the magneto-dynamic force to the resistance force induced by the viscoelastic stress of the suspension, a dimensionless parameter defined as magnetic yield parameter [9] can be obtained:

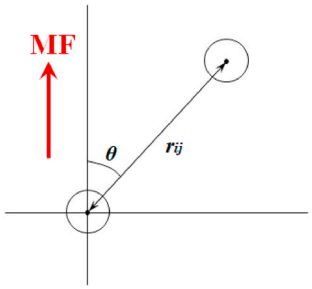

Fig. 11. Schematic diagram of two magnetic nanoparticles in a homogeneous magnetic field.

$$Y_M = \frac{F_{particle}}{F_{viscous}} = \frac{F_{particle}}{\pi d^2 \cdot \tau_{vs}} = \frac{\mu_0(\rho M)^2}{24\tau_{vs}} \cdot \left(\frac{d}{r_{ij}}\right)^4 \tag{5}$$

Assuming that all the nanoparticles are arranged in the voids between cement particles as cubic order with same inter-particle distance (h (m)), as presented in Fig. 12, the volume fraction of the nanoparticles with average particle size of d in a cubic cell is defined as:

$$\varphi_{MNPs} = \frac{V_{particle}}{V_{cell}} = \frac{\frac{4}{3}\pi\left(\frac{d}{2}\right)^3}{(d+h)^3} = \frac{\pi}{6}\cdot\left(\frac{d}{d+h}\right)^3 \tag{6}$$

Thus, the center distance between two neighboring magnetic nanoparticles is expressed as:

$$r_{ij} = d + h = d\cdot\left(\frac{\pi}{6\varphi_{MNPs}}\right)^{\frac{1}{3}} \tag{7}$$

Substituting Eq. (7) in the above Eq. (5), the magnetic yield parameter can be modified as follows:

$$Y_M^* = \frac{\mu_0(\rho M)^2}{24\tau_{vs}} \cdot \left(\frac{6\varphi_{MNPs}}{\pi}\right)^{\frac{4}{3}} \tag{8}$$

where τ_{vs} is the viscoelastic stress of the suspension (Pa). The volume fraction of the nanoparticles in the voids between cement particles (φ_{MNPs}) can be calculated by the following equation:

$$\varphi_{MNPs} = \frac{V_{MNPs}}{(1-\varphi_C)\cdot V_{Total}} \tag{9}$$

where φ_C is the volume fraction of cement (%). V_{MNPs} and V_{total} are the volume of nanoparticles and total paste (kg/m^3), respectively. Theoretically, when $Y_M^* > 1$, the magneto-dynamic force is higher than the resistance force, magnetic chains or clusters can be formed and the suspension will show significant magneto-rheological response, while $Y_M^* < 1$ means that the suspension prevents the formation of clusters structure [11]. It can be clearly seen that the magnitude of the modified magnetic yield parameter depends on the concentration and physical properties of the nanoparticles as well as the viscoelastic stress of the suspension.

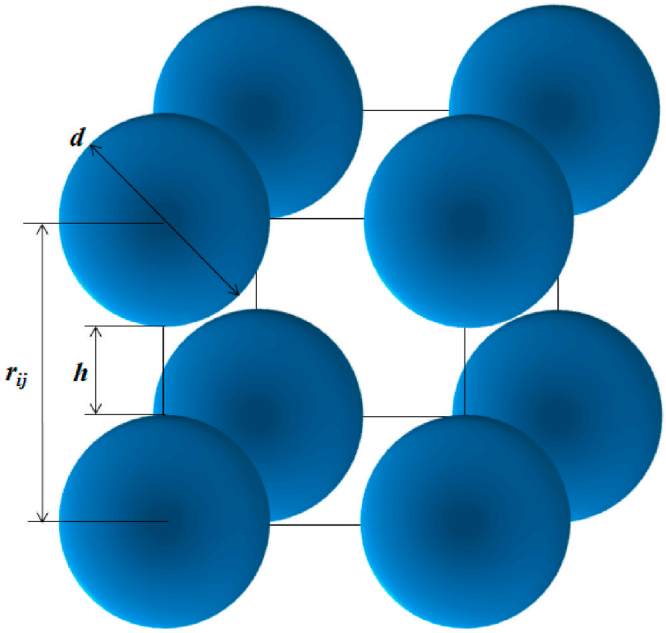

Fig. 12. Schematic diagram of cubic-order arrangement of nanoparticles in the voids between cement particles.

4.2. Movement velocity of magnetic nanoparticles

For a spherical particle settling in a Bingham plastic fluid under gravitational force, He et al. [44] derived the viscous drag equation which can be expressed as:

$$F_D = 3\pi d^2\left[\frac{\eta_{pl}v}{d}+\tau_{pl}\right] \tag{10}$$

The equilibrium velocity of the spherical particle can be calculated by equating the gravitational and buoyant force to the viscous drag equation. In the case of nano-Fe_3O_4 incorporated cement paste under an external magnetic field, the magnetic force plays a comparable role to the gravitational force. When the magnetic force is higher than the resistance induced by the viscoelastic stress of the suspension ($Y_M^* > 1$), similarly, the magnetic nanoparticles in equilibrium can be considered to move at constant velocity in the interstitial medium. Assuming that the flow behavior induced by magnetic field follows Bingham law, the equilibrium velocity can be estimated by equalizing magnitude the magneto-dynamic force and the drag force:

$$\frac{\pi d^2\mu_0(\rho M)^2}{24}\cdot\left(\frac{6\varphi_{MNPs}}{\pi}\right)^{\frac{4}{3}} = 3\pi d^2\left(\frac{\eta_{pl}v}{d}+\tau_{pl}\right) \tag{11}$$

Or in an explicit way as:

$$v = \frac{d}{\eta_{pl}}\left[\frac{\mu_0(\rho M)^2}{72}\cdot\left(\frac{6\varphi_{MNPs}}{\pi}\right)^{\frac{4}{3}}-\tau_{pl}\right] \tag{12}$$

where v is the movement velocity of nanoparticles (m/s), τ_{pl} and η_{pl} are the Bingham yield stress (Pa) and the plastic viscosity (Pa.s) of the suspension, respectively. It can be seen that the estimated movement velocity of a magnetic nanoparticle in cement-based suspensions is dependent on the properties of the nanoparticles (particle size, density, concentration and magnetic properties) and the Bingham yield stress and plastic viscosity of the paste. Again, the conceptual velocity estimation is considered as an indicator representing the movement between two neighboring nanoparticles, not the actual evolving velocity while moving in the suspension.

5. Discussion

According to our hypothesis, the moving magnetic nanoparticles immediately after application of the external magnetic field destroy the early C-S-H links between cement particles and then agglomerate to form chains or clusters. The intensity of C-S-H bridges between cement grains can be characterized by the smallest critical strain with several hundredths of % [39]. Given the rapid response time of cement pastes with nano-Fe_3O_4 to a magnetic field, the elastic limit yield stress corresponding to the end of the linear viscoelastic region (without magnetic field) is selected as the viscoelastic stress of the paste in Eq. (8) to calculate the magnetic yield parameter. When the magneto-dynamic force overcomes the contacts between cement particles, the cement paste is postulated to exhibit slight flow behavior due to the micro-agitation effect of the moving nanoparticles. In other words, the shear rate of the flowing paste induced by the magnetic force is regarded to be small-scale. In this case, the viscosity at linear low shear rate region is selected for the calculation of the movement velocity of the nanoparticles. For the Bingham yield stress in Eq. (12), it could be selected from the following calculations. Based on Eq. (8), the critical magnetic yield parameter (i.e. $Y_M^* = 1$) is derived as:

$$\tau_{ys} = \frac{\mu_0(\rho M)^2}{24}\cdot\left(\frac{6\varphi_{MNPs}}{\pi}\right)^{\frac{4}{3}} \tag{13}$$

At zero movement velocity, the critical Bingham yield stress can be derived as:

$$\tau_{pl} = \frac{\mu_0(\rho M)^2}{72}\cdot\left(\frac{6\varphi_{MNPs}}{\pi}\right)^{\frac{4}{3}} \tag{14}$$

For reasons of consistency, having a zero velocity in the case of $Y_M^* = 1$, the term τ_{pl} in Eq. (12) is thus assumed to be one third of the elastic limit yield stress where the breakage of C-S-H bridges occurs. Based on the aforementioned assumptions and selections of relevant parameters, the estimated magnetic yield parameter and movement velocity of nanoparticles for all the cement pastes under magnetic field of 0.5 T are listed in Table 4.

For the cement paste with w/c of 0.4 and nano-Fe_3O_4 particles of 3 wt%, it can be clearly seen that the magnetic yield parameter is much larger than 1 and the movement velocity of the nanoparticles is sufficiently large compared to the estimated average distance between neighboring nanoparticles (h). This indicates that the nano-Fe_3O_4 particles can move to connect with each other in a very short time if a magnetic field with 0.5 T was applied. The calculated parameters provide a valuable evidence for the fast movement of nano-Fe_3O_4 particles in the cement paste under the magnetic field of 0.5 T. Reducing w/c resulted in a decrease in the magnetic yield parameter and the movement velocity, indicating that it is more difficult for nanoparticles to form magnetic clusters. The magnetic yield parameter of cementitious paste with 0.2% PCE was lower than 1, indicating that the nano-Fe_3O_4 particles are hardly to move in the paste medium under the magnetic field with 0.5 T. For cement paste with higher PCE content, taking 0.6% as an example, the magnetic yield parameter was slightly higher than 1. This indicates that some nano-Fe_3O_4 particles were able to break down the C-S-H bridges between cement particles and the cement paste could exhibit rheological response to the external magnetic field. All the calculated parameters are in good agreement with the experimental results. The calculated magnetic yield parameter and movement velocity are useful indicators to describe the extent of magneto-rheological responses of cement paste containing nano-Fe_3O_4 particles.

6. Conclusions

In the present study, the magneto-rheological responses of cement paste with nano-Fe_3O_4 particles as well as the influences of cement paste medium were investigated. Conceptual equations about magneto-dynamic force and movement velocity of nanoparticles dispersed in cement paste were derived. Based on the results and discussion, the following conclusions can be reached:

(1) Applying an external magnetic field promotes nano-Fe_3O_4 particles to form chains or clusters, creating a sort of mechanical micro-agitation effect. This action probably destroys early C-S-H bridges between cement particles, further releasing entrained water in agglomerated cement clusters. Therefore, cement paste containing nano-Fe_3O_4 particles shows liquid-like behavior immediately after initiation of the external magnetic field.
(2) After longer magnetization period, cement paste with nano-Fe_3O_4 particles gradually transitions from viscous state to elastic state, most probably due to the improvement of interactions between

Table 4
Estimated magnetic yield parameter and movement velocity of nanoparticles.

Mix.	M (0.5 T)/ (Am^2/kg)	$\tau_{c,ys}$/ (Pa)	η_{pl}/(Pa. s)	h/ (nm)	Y_M^*	v/(10^{-9} m/s)
0.4	49.43	4.52	7.21	48.30	9.38	43.79
0.35	49.43	5.99	10.65	46.02	8.04	32.98
0.35 + 0.2%PCE	49.43	59.91	20.00	46.12	0.80	–
0.35 + 0.4%PCE	49.43	45.03	28.89	46.23	1.06	0.73
0.35 + 0.6%PCE	49.43	19.22	9.44	46.33	2.46	24.79

magnetic clusters and the regeneration of C-S-H bridges between cement particles. The cement paste containing magnetic nanoparticles under an external magnetic field shows enhanced stiffness compared to the paste without magnetic field owing to the presence of magnetic clusters.

(3) Without superplasticizer, the magneto-rheological responses of cement paste containing nano-Fe_3O_4 particles are weakened with the decrease of w/c. At fixed w/c, the cement paste with low dosage of PCE shows negligible magneto-rheological responses due to the high elastic limit yield stress and viscosity of the cement paste.

(4) The estimated magnetic yield parameter and the movement velocity of the nanoparticles in cement-based suspensions under magnetic field can be used as relevant indicators to describe the extent of magneto-rheological responses of cement paste containing nano-Fe_3O_4 particles.

Declaration of competing interest

The authors declared that we have no conflicts of interest to this work. We declare that we do not have any commercial or associative interest that represents a conflict of interest in connection with the work submitted.

Acknowledgements

This paper is a deliverable of the ERC Advanced Grant project 'SmartCast'. This project has received funding from the European Research Council (ERC) under the European Union's Horizon 2020 research and innovation program (grant agreement No. 693755). The authors gratefully acknowledge the financial support received from ERC.

References

[1] G. De Schutter, Thixotropic Effects during Large-Scale Concrete Pump Tests on Site, 71st RILEM Annual Week & ICACMS 2017Chennai, India, 2017.
[2] N. Roussel, F. Cussigh, Distinct-layer casting of SCC: the mechanical consequences of thixotropy, Cement Concr. Res. 38 (2008) 624–632.
[3] G. Ovarlez, N. Roussel, A physical model for the prediction of lateral stress exerted by self-compacting concrete on formwork, Mater. Struct. 39 (2006) 269–279.
[4] N. Roussel, A thixotropy model for fresh fluid concretes: theory, validation and applications, Cement Concr. Res. 36 (2006) 1797–1806.
[5] G. De Schutter, K. Lesage, Active control of properties of concrete: a (p)review, Mater. Struct. 51 (2018) 123.
[6] G. De Schutter, K. Lesage, V. Mechtcherine, V.N. Nerella, G. Habert, I. Agusti-Juan, Vision of 3D printing with concrete - technical, economic and environmental potentials, Cement Concr. Res. 112 (2018) 25–36.
[7] I. Bica, Y.D. Liu, H.J. Choi, Physical characteristics of magnetorheological suspensions and their applications, J. Ind. Eng. Chem. 19 (2013) 394–406.
[8] M. Ashtiani, S.H. Hashemabadi, A. Ghaffari, A review on the magnetorheological fluid preparation and stabilization, J. Magn. Magn Mater. 374 (2015) 716–730.
[9] P.J. Rankin, A.T. Horvath, D.J. Klingenberg, Magnetorheology in viscoplastic media, Rheol. Acta 38 (1999) 471–477.
[10] Y. Yang, L. Li, G. Chen, Static yield stress of ferrofluid-based magnetorheological fluids, Rheol. Acta 48 (2009) 457–466.
[11] J.P. Rich, P.S. Doyle, G.H. McKinley, Magnetorheology in an aging, yield stress matrix fluid, Rheol. Acta 51 (2012) 579–593.
[12] D. Susan-Resiga, L. Vékás, Yield stress and flow behavior of concentrated ferrofluid-based magnetorheological fluids: the influence of composition, Rheol. Acta 53 (2014) 645–653.
[13] G.H. Tattersall, P.F. Banfill, The Rheology of Fresh Concrete, 1983.
[14] M.A. Schultz, L.J. Struble, Use of oscillatory shear to study flow behavior of fresh cement paste, Cement Concr. Res. 23 (1993) 273–282.
[15] D. Jiao, C. Shi, Q. Yuan, X. An, Y. Liu, H. Li, Effect of constituents on rheological properties of fresh concrete-A review, Cement Concr. Compos. 83 (2017) 146–159.
[16] M.S. Choi, Y.S. Kim, J.H. Kim, J.-S. Kim, S.H. Kwon, Effects of an externally imposed electromagnetic field on the formation of a lubrication layer in concrete pumping, Construct. Build. Mater. 61 (2014) 18–23.
[17] I. Abavisani, O. Rezaifar, A. Kheyroddin, Alternating magnetic field effect on fine-aggregate steel chip–reinforced concrete properties, J. Mater. Civ. Eng. 30 (2018), 04018087.
[18] A.M. Rashad, A synopsis about the effect of nano-Al2O3, nano-Fe2O3, nano-Fe3O4 and nano-clay on some properties of cementitious materials – a short guide for Civil Engineer, Mater. Des. 52 (2013) 143–157.
[19] H. Li, H.-g. Xiao, J. Yuan, J. Ou, Microstructure of cement mortar with nano-particles, Compos. B Eng. 35 (2004) 185–189.
[20] M.S. Amin, S.M.A. El-Gamal, F.S. Hashem, Effect of addition of nano-magnetite on the hydration characteristics of hardened Portland cement and high slag cement pastes, J. Therm. Anal. Calorim. 112 (2012) 1253–1259.
[21] A.H. Shekari, M.S. Razzaghi, Influence of nano particles on durability and mechanical properties of high performance concrete, Procedia Engineering 14 (2011) 3036–3041.
[22] M.O.G.P. Bragança, K.F. Portella, M.M. Bonato, E. Alberti, C.E.B. Marino, Performance of Portland cement concretes with 1% nano-Fe3O4 addition: electrochemical stability under chloride and sulfate environments, Construct. Build. Mater. 117 (2016) 152–162.
[23] I. Mansouri, M. Nejat, S. Shahbazi, A. Karami, Effect of Magnetite Nanoparticles (Ferroferric Oxide) on Discrete Concrete Properties, Proceedings of the Institution of Civil Engineers-Construction Materials, 2018, pp. 1–8.
[24] D. Jiao, K. El Cheikh, K. Lesage, C. Shi, G. De Schutter, Structural Build-Up of Cementitious Paste under External Magnetic Fields, Rheology and Processing of Construction Materials, 2019, pp. 36–42. Springer.
[25] D. Jiao, K. El Cheikh, C. Shi, K. Lesage, G. De Schutter, Structural build-up of cementitious paste with nano-Fe3O4 under time-varying magnetic fields, Cement Concr. Res. 124 (2019), 105857.
[26] EN TS 196-1, Methods of Testing Cement–Part 1: Determination of Strength, European Committee for standardization, 2005, p. 26.
[27] S.D. Nair, R.D. Ferron, Set-on-demand concrete, Cement Concr. Res. 57 (2014) 13–27.
[28] D. Jiao, C. Shi, K. Lesage, K. El Cheikh, G. De Schutter, Rheological Behavior of Cement Paste under Magnetic Field, National Civil Engineering Forum for Graduate Students (NCEF2018), 2018.
[29] N.M. Wereley, A. Chaudhuri, J.H. Yoo, S. John, S. Kotha, A. Suggs, R. Radhakrishnan, B.J. Love, T.S. Sudarshan, Bidisperse magnetorheological fluids using Fe particles at nanometer and micron scale, J. Intell. Mater. Syst. Struct. 17 (2006) 393–401.
[30] Y.D. Liu, H.J. Choi, Magnetorheology of core–shell typed dual-coated carbonyl iron particle fabricated by a sol–gel and self-assembly process, Mater. Res. Bull. 69 (2015) 92–97.
[31] D. Feys, R. Verhoeven, G. De Schutter, Why is fresh self-compacting concrete shear thickening? Cement Concr. Res. 39 (2009) 510–523.
[32] A. Yahia, Effect of solid concentration and shear rate on shear-thickening response of high-performance cement suspensions, Construct. Build. Mater. 53 (2014) 517–521.
[33] D. Jiao, C. Shi, Q. Yuan, Influences of shear-mixing rate and fly ash on rheological behavior of cement pastes under continuous mixing, Construct. Build. Mater. 188 (2018) 170–177.
[34] D. Jiao, C. Shi, Q. Yuan, Time-dependent rheological behavior of cementitious paste under continuous shear mixing, Construct. Build. Mater. 226 (2019) 591–600.
[35] B. Feneuil, O. Pitois, N. Roussel, Effect of surfactants on the yield stress of cement paste, Cement Concr. Res. 100 (2017) 32–39.
[36] Y. Qian, K. Lesage, K. El Cheikh, G. De Schutter, Effect of polycarboxylate ether superplasticizer (PCE) on dynamic yield stress, thixotropy and flocculation state of fresh cement pastes in consideration of the Critical Micelle Concentration (CMC), Cement Concr. Res. 107 (2018) 75–84.
[37] A.M. Mostafa, A. Yahia, New approach to assess build-up of cement-based suspensions, Cement Concr. Res. 85 (2016) 174–182.
[38] Q. Yuan, X. Lu, K.H. Khayat, D. Feys, C. Shi, Small amplitude oscillatory shear technique to evaluate structural build-up of cement paste, Mater. Struct. 50 (2017) 112.
[39] N. Roussel, G. Ovarlez, S. Garrault, C. Brumaud, The origins of thixotropy of fresh cement pastes, Cement Concr. Res. 42 (2012) 148–157.
[40] N. Roussel, A. Gram, Simulation of Fresh Concrete Flow, vol. 15, RILEM State-of-the-Art Reports, 2014.
[41] D. Jiao, K. Lesage, M.Y. Yardimci, K. El Cheikh, C. Shi, G. De Schutter, Quantitative assessment of the influence of external magnetic field on clustering of nano-Fe3O4 particles in cementitious paste, Cement Concr. Res. 142 (2021) 106345.
[42] S.P. Jiang, J.C. Mutin, A. Nonat, Studies on mechanism and physico-chemical parameters at the origin of the cement setting. I. The fundamental processes involved during the cement setting, Cement Concr. Res. 25 (1995) 779–789.
[43] S.D. Nair, R.D. Ferron, Real time control of fresh cement paste stiffening: smart cement-based materials via a magnetorheological approach, Rheol. Acta 55 (2016) 571–579.
[44] Y.B. He, J.S. Laskowski, B. Klein, Particle movement in non-Newtonian slurries: the effect of yield stress on dense medium separation, Chem. Eng. Sci. 56 (2001) 2991–2998.